

**Wave packet revivals and the energy eigenvalue spectrum  
of the quantum pendulum**

M. A. Doncheski\*

*Department of Physics*

*The Pennsylvania State University*

*Mont Alto, PA 17237 USA*

R. W. Robinett†

*Department of Physics*

*The Pennsylvania State University*

*University Park, PA 16802 USA*

(Dated: October 20, 2018)

arXiv:quant-ph/0307079v1 10 Jul 2003

## Abstract

The rigid pendulum, both as a classical and as a quantum problem, is an interesting system as it has the exactly soluble harmonic oscillator and the rigid rotor systems as limiting cases in the low- and high-energy limits respectively. The energy variation of the classical periodicity ( $\tau$ ) is also dramatic, having the special limiting case of  $\tau \rightarrow \infty$  at the 'top' of the classical motion (i.e. the separatrix.) We study the time-dependence of the quantum pendulum problem, focusing on the behavior of both the (approximate) classical periodicity and especially the quantum revival and superrevival times, as encoded in the energy eigenvalue spectrum of the system. We provide approximate expressions for the energy eigenvalues in both the small and large quantum number limits, up to 4th order in perturbation theory, comparing these to existing handbook expansions for the characteristic values of the related Mathieu equation, obtained by other methods. We then use these approximations to probe the classical periodicity, as well as to extract information on the quantum revival and superrevival times. We find that while both the classical and quantum periodicities increase monotonically as one approaches the 'top' in energy, from either above or below, the revival times decrease from their low- and high-energy values until very near the separatrix where they increase to a large, but finite value.

PACS numbers: 03.65.Ge, 03.65.Sq

---

\*Electronic address: mad10@psu.edu

†Electronic address: rick@phys.psu.edu

## I. INTRODUCTION

The problem of a point particle, restricted to a circular radius, and subject to a uniform gravitational (or electric) field, namely a rigid pendulum, is one of the most familiar of all problems in classical mechanics. The corresponding quantum version was first considered early in the history of quantum mechanics by Condon [1] and is sometimes discussed in the more physical context of hindered internal rotations [2] - [5] in chemistry. The problem is also a staple of the pedagogical literature [6] - [8] and is often seen as an example of perturbation theory methods [9] - [11], especially in collections of problems in quantum mechanics [12] - [17], where is often described as the plane rotator in an electric field. Most treatments focus attention on aspects of the structure of the energy eigenvalues spectrum, with only a handful (see, *e.g.*, [7]) examining the question of time-dependence of wave packet solutions.

More recently, the realization that important information on longer-term quantum correlations, in the form of wave packet revivals and superrevivals, is also encoded in the energy eigenvalue spectrum, has focused new attention on the time dependence of physical and model systems which exhibit such interesting dynamics. In many such systems, initially localized states which have a short-term, quasi-classical time evolution, can spread significantly over several orbits, only to reform later in the form of a quantum revival in which the spreading reverses itself, the wave packet relocalizes, and the semi-classical periodicity is once again evident. Such revival phenomena have been observed in a wide variety of physical systems, especially in Rydberg atoms [18], [19], and calculations exist for many other model systems [20].

The archetype of a one-dimensional model system for quantum revivals is the infinite well (where such revivals are exact) and a number of analyses [21] - [26] have provided insight into both the short-term and long-term behavior of wave packets. The rigid rotor, which like the infinite well, also has an  $n^2$  quantum number dependence in the energy spectrum, behaves very similarly [24], [27], with neither system exhibiting higher-order correlations (such as superrevivals) due to the simplicity of their energy level structure. Harmonic oscillator systems, with a simple spectrum proportional to  $n$ , do not exhibit quantum revivals (or rather have  $T_{rev} \rightarrow \infty$ ), or super-revivals, but Morse-type generalizations [28], [29], with anharmonic terms present, have predictable revival structures, as confirmed in observations of molecular systems [30]. One-dimensional power-law potentials of the form  $V_{(k)}(x) =$

$V_0|x/L|^k$  also provide examples [31] of interesting quantum revival time behavior as a model parameter is varied, as they interpolate between the cases of the oscillator ( $k = 2$ ) and infinite well ( $k \rightarrow \infty$ ) limits.

For many such systems, which depend on a single quantum number, one typically expands the energy eigenvalues (assuming integral values) about the central value used in the construction of a wave packet via

$$E(n) \approx E(n_0) + E'(n_0)(n - n_0) + \frac{1}{2}E''(n_0)(n - n_0)^2 + \frac{1}{6}E'''(n_0)(n - n_0)^3 + \dots \quad (1)$$

in terms of which the classical period, revival, and superrevival times are given respectively by

$$\tau \equiv T_{cl} = \frac{2\pi\hbar}{|E'(n_0)|} \quad , \quad T_{rev} = \frac{2\pi\hbar}{|E''(n_0)|/2} \quad , \quad T_{super} = \frac{2\pi\hbar}{|E'''(n_0)|/6} \quad (2)$$

so that information on the long-term quantum correlations present in many wave packet solutions is encoded in the energy spectrum, just as is the short-term quasi-classical time-dependence. In typical experimental realizations of such systems, one finds  $\tau \ll T_{rev} \ll T_{super}$ .

In this report, we will focus on the structure of the quantum revival (and superrevival) time for the problem of the quantum pendulum, extending earlier analyses of the approximate energy spectrum for this problem, in both the low- and high-energy limits, as well as making use of numerically obtained values for the entire spectrum. We are interested in such questions as (i) what is the revival time,  $T_{rev}$  for the (anharmonic) oscillator limit of the quantum pendulum and (ii), how do the quantum revival and superrevival times vary (from both the low-energy oscillator and high-energy rotor limits) as one approaches energies near the separatrix value. To probe such questions, we begin, in Sec. II by defining the generic problem of the quantum pendulum, and review standard expressions for the energy dependence of the classical periodicity of the pendulum,  $\tau(E)$  versus  $E$ . We then discuss, in Sec. III, the quantum version of this problem, reviewing its equivalence to the Mathieu equation of the mathematical physics literature, and making contact with 'handbook' results for its periodic solutions from standard references. In Secs. IV and V, we discuss perturbative solutions to the quantum pendulum problem, in the high energy (free rotor) and low energy (oscillator like) limits respectively, deriving results up to 4th order in perturbation theory. We use these results to discuss the classical periodicity, as well as the quantum revivals and superrevivals in these two limiting cases. Finally, we use these earlier results

as benchmarks against which to compare the numerical evaluation of the energy eigenvalues for the pendulum over the entire spectrum, focusing on the behavior of  $T_{rev}$  and  $T_{super}$  near the 'top' of the pendulum. Some of the mathematical details of the high-energy limit are discussed in a WKB-approximation in Appendix A, while the details of the perturbative expansion in the low-energy, oscillator-like limit are given in Appendix B.

## II. CLASSICAL BACKGROUND

For definiteness, we will consider a point particle of mass  $\mu$  (a notation used to avoid confusion with familiar angular momentum quantum numbers) restricted to a circle of radius  $l$ , which therefore has a rotational inertia  $I \equiv \mu l^2$ . It is subject to either a uniform gravitational ( $mg$ ) or electric ( $QE$ ) force in the vertical direction, giving rise to a potential energy function of the form

$$V(\theta) = -V_0 \cos(\theta) \quad \text{where} \quad V_0 = \begin{cases} mgl & \text{(quantum pendulum)} \\ QEl & \text{(Stark effect for rigid rotor)} \end{cases}. \quad (3)$$

(One can also consider a point electric dipole,  $p$ , in a uniform electric field, in which case  $V_0 = pE$ .)

We can rewrite the classical conservation of energy connection

$$\frac{I}{2} \left( \frac{d\theta}{dt} \right)^2 - V_0 \cos(\theta) = E \quad (4)$$

in the form

$$\frac{d\theta}{dt} = \sqrt{\frac{2}{I}} \sqrt{E + V_0 \cos(\theta)} \quad (5)$$

or

$$\sqrt{\frac{I}{2}} \frac{d\theta}{\sqrt{E + V_0 \cos(\theta)}} = dt \quad (6)$$

which can, of course, be formally integrated in terms of elliptic integrals (or evaluated numerically) to obtain  $\theta(t)$  solutions.

For energies satisfying  $-V_0 < E < +V_0$ , the motion will be periodic with classical turning points at  $\pm\Theta = \pm \cos^{-1}(-E/V_0)$  and the classical period is given by

$$\tau(E) = 2\sqrt{\frac{I}{2}} \int_{-\Theta}^{+\Theta} \frac{d\theta}{\sqrt{E + V_0 \cos(\theta)}} \quad (7)$$

where the extra factor of 2 comes from including both the 'back' and the 'forth' motions. For low energies, in the limit of small oscillations, with  $-V_0 \lesssim E \ll +V_0$  or  $\Theta \ll 1$ , the motion is oscillator like with an energy independent period given by  $\tau = 2\pi/\sqrt{V_0/I}$ . In the  $E \rightarrow +V_0$  (or separatrix) limit, the classical period diverges logarithmically.

For the case of unbounded motion, where  $E > +V_0$ , one period corresponds more simply to a single revolution, with the result

$$\tau(E) = \sqrt{\frac{I}{2}} \int_{-\pi}^{+\pi} \frac{d\theta}{\sqrt{E + V_0 \cos(\theta)}} \quad (8)$$

and in the high-energy (rotor-like) limit, when  $E \equiv I\Omega^2/2 \gg +V_0$ , we find that

$$\tau \rightarrow \sqrt{\frac{I}{2}} \frac{2\pi}{\sqrt{E}} = \frac{2\pi}{\Omega} \quad (9)$$

as expected. The expressions in Eqn. (7) and (8) for  $\tau(E)$  versus  $E$  can then be compared to the corresponding quantum values of  $\tau_n(E_n)$  versus  $E_n$  in the appropriate limiting cases.

### III. SCHRÖDINGER EQUATION FOR THE QUANTUM PENDULUM AND MATHIEU EQUATION

The Schrödinger equation for the quantum pendulum can be written in terms of the moment of inertia,  $I$ , in the form

$$\frac{\hat{p}_\theta^2}{2I} \psi(\theta) + V(\theta)\psi(\theta) = -\frac{\hbar^2}{2I} \frac{d^2\psi(\theta)}{d\theta^2} - V_0 \cos(\theta)\psi(\theta) = E\psi(\theta). \quad (10)$$

The conventional change of variables,  $\theta \equiv 2z$ , can be used to rewrite this as

$$\frac{d^2\psi(z)}{dz^2} + \left[ \frac{8IE}{\hbar^2} + \frac{8IV_0}{\hbar^2} \cos(2z) \right] \psi(z) \quad (11)$$

which is recognizable as a familiar equation of mathematical physics,

$$\frac{d^2\psi(z)}{dz^2} + [a + 2q \cos(z)]\psi(z) \quad (12)$$

namely Mathieu's equation [32], [33] (with  $q \rightarrow -q$  in this case) and where we identify

$$q \equiv \frac{4IV_0}{\hbar^2} \quad \text{and} \quad a \equiv \frac{8IE}{\hbar^2}. \quad (13)$$

Because of the intrinsic parity of the potential, the solutions can be characterized as being even,  $ce_r(z, q)$  or cosine-like, or odd,  $se_r(z, q)$  or sine-like, for integral values of  $r$ , with  $r \geq 0$

( $r \geq 1$ ) for even (odd) cases. For the limiting case of  $q = 0$ , the solutions (in standard normalization [32], [33]) have the forms

$$ce_0(z, 0) = 1/\sqrt{2} \quad r = 0 \quad (14)$$

$$ce_r(z, 0) = \cos(rz) \quad r \geq 1 \quad (15)$$

$$se_r(z, 0) = \sin(rz) \quad r \geq 1. \quad (16)$$

For a fixed value of  $q$ , only for specific (or in more standard notation, characteristic) values of the parameter  $a$  will the solutions be periodic, with periods of  $\pi$  or  $2\pi$  in the variable  $z$ , and these are denoted by  $a_r, b_r$  for the even and odd solutions respectively. For each value of  $q$ , there are countably infinite number of solutions, labeled by  $r$ . For the physical case considered here, where the system must exhibit  $2\pi$  periodicity in the variable  $\theta$ , one chooses the even integer ( $r = 2m$ )  $ce_{2m}(z, q)$  and  $se_{2m}(z, q)$  solutions which have period  $\pi$  in the variable  $z$ . Standard mathematical packages (such as *Mathematica*<sup>®</sup>) can quickly evaluate the characteristic values for a given value of  $q$  and we plot in Fig. 1 the pattern of characteristic values  $a_{2m}$  (solid curves for the even solutions) and  $b_{2m}$  (dashed curves for the odd solutions) which are proportional to the allowed quantized energies,  $E$ , for different values of  $q$ , corresponding to increasing values of  $V_0$ . For  $E \gg +V_0$  ( $a \gg q$ ), the solutions are doubly degenerate corresponding to the free rotor limit: in this case, the real  $ce_{2m}$  and  $se_{2m}$  solutions are analogous to linear combinations of clockwise ( $\exp(im\theta)$ ) and counterclockwise ( $\exp(-im\theta)$ ) rotational eigenstates of the plane rotator. For  $-V_0 < E \ll +V_0$ , the spectrum splits into equally spaced oscillator like states corresponding to the quantized version of small angle isochronous oscillations.

Standard mathematical references [32], [33] provide approximations for the characteristic values,  $a_r, b_r$ , as a function of  $q$  in both the  $q \ll 1$  and  $q \gg 1$  limits, typically derived by expanding the solutions in appropriate Fourier-like series expansions. For the 'high energy' or rotor limit, with  $q \ll 1$ , one finds (for  $r \gtrsim 7$ ) that the  $a_r, b_r$  are approximately degenerate with

$$\left. \begin{array}{l} a_r \\ b_r \end{array} \right\} = r^2 + \frac{q^2}{2(r^2 - 1)} + \frac{(5r^2 + 7)q^4}{32(r^2 - 1)^3(r^2 - 4)} + \dots \quad (17)$$

and the difference between the characteristic values for even and odd solutions is known to satisfy

$$a_r - b_r = \mathcal{O}(q^r/r^{r-1}) \quad \text{as} \quad r \rightarrow \infty. \quad (18)$$

In the other limiting case, when  $q \gg 1$  and the spectrum is approximately oscillator like, and one finds

$$a \approx -2q + 2p\sqrt{q} - \frac{(p^2 + 1)}{2^3} - \frac{(p^3 + 3p)}{2^7\sqrt{q}} - \frac{(5p^4 + 34p^2 + 9)}{2^{12}q} - \frac{(33p^5 + 410p^3 + 405p)}{2^{17}q^{3/2}} - \dots \quad (19)$$

where  $p \equiv 2n + 1$  which has the clear  $(n + 1/2)\hbar\omega$  oscillator dependence in low order. We will explicitly show, in Sec. V and Appendix B, how this expansion arises using perturbation theory, at least up to 4th-order, including all of the terms shown above. We note that handbook expansions exist to sixth-order (in both the low- and high-energy limits), so that one could improve on the explicit quantum mechanical perturbative calculations discussed below by using these results.

While we will focus on approximate perturbative results in the next two sections, when we do compare to purely numerical results, we will make use of the following nominal set of parameter values,

$$\hbar = 2\mu = l = 1 \quad \text{and} \quad V_0 = 80 \quad (20)$$

corresponding to  $q = 160$ . This choice can be seen, from Fig. 1, to exhibit a large number of oscillator like states below the  $+V_0$  threshold. For these parameter values, *Mathematica*<sup>®</sup> returns characteristic values with the equivalent of double-precision accuracy.

#### IV. HIGH ENERGY ROTOR LIMIT

In the limit of vanishing gravitational or electric field, the quantum pendulum reduces to a free rotor with Schrödinger equation and solutions given by

$$-\frac{\hbar^2}{2I} \frac{d^2\psi_m(\theta)}{d\theta^2} = E_m^{(0)}\psi_m(\theta) \quad \text{with} \quad \psi_m(\theta) = \frac{1}{\sqrt{2\pi}}e^{im\theta} \quad \text{and} \quad E_m^{(0)} = \frac{\hbar^2 m^2}{2I} \quad (21)$$

with  $m = 0, \pm 1, \pm 2, \dots$ . The solutions with  $+m, -m$  for  $|m| \neq 0$  are degenerate, corresponding to the equivalence of clockwise and counter clockwise motions. Linear combinations of these solutions can be used to obtain eigenfunctions of definite parity as

$$\Theta_m(\theta) = \begin{cases} 1/\sqrt{2\pi} & \text{for } m = 0 \\ \cos(m\theta)/\sqrt{\pi} & \text{for } m > 0 \\ \sin(m\theta)/\sqrt{\pi} & \text{for } m < 0 \end{cases} \quad (22)$$

The classical period associated with this zeroth-order result requires

$$\frac{dE_m}{dm} \equiv E'_m = \frac{\hbar^2 m}{I} = \hbar \sqrt{\frac{2E_m}{I}} \quad (23)$$



so that

$$\tau_m^{(0)} \equiv \frac{2\pi\hbar}{|E'_m|} = 2\pi/\sqrt{2E_m^{(0)}/I} \quad (24)$$

which is consistent with the purely classical result of Eqn. (9). The corresponding revival time is

$$T_{rev} = \frac{2\pi\hbar}{|E''_m/2|} = \frac{4\pi I}{\hbar}. \quad (25)$$

These simple results can therefore be used to obtain zeroth-order approximations for the quantized energies, classical periods, and revival times in the large-energy rotor limit. We note that in leading order, the superrevival and all higher-order correlation times diverge due to the simple quadratic dependence on quantum number, just as for the one-dimensional infinite well.

Using the standard set of values in Eqn. (20), we first exhibit the zeroth order energy eigenvalue predictions (compared to the 'numerically exact' results) in Fig. 2, and then compare the  $\tau_m^{(0)}$  versus  $E_m^{(0)}$  values to the classical periodicity in Fig. 3 in this same limit. Finally, in Fig. 4, we illustrate the predictions for the revival time,  $T_{rev}$  versus  $E_m$ .

The effect of a constant external field (Stark effect) on the spectrum of the rotor is a well-known example of second-order degenerate perturbation theory [9] - [17] and the general result for the second-order energy shift is

$$E_{(m)}^{(2)} = \frac{IV_0^2}{\hbar^2(4m^2 - 1)} \quad (26)$$

for both even and odd states. Note that the first-order, and all odd-order shifts vanish for symmetry reasons. The special case of  $|m| = 1$  must be treated separately with the result that the  $+1, -1$  states are split to this order [9] - [10], [16], [17]. More generally, it can be argued [6] that the degeneracy in  $a_r, b_r$  is split in  $r$ -th order in perturbation theory, as in Eqn. (18). When this result (Eqn. (26)) is written in terms of the parameters  $a$  and  $q$ , it reproduces the next-to-leading order of the 'handbook' expansion in Eqn. (17) to  $\mathcal{O}(q^2)$ .

This next-to-leading term then provides important corrections not only to the energy eigenvalues (especially for lower energy, smaller  $m$  states), but also to the quantum expressions for the classical period (via  $|E'_m|$ ) and the revival time (via  $|E''_m|$ ). Including these next-to-leading order results gives the second order predictions (shown as boxes) for these quantities in Figs. 2, 3, and 4. We note that the quantum revival times decrease from their high-energy value in Eqn. (25) as one approaches the critical  $E \sim +V_0$  value from above;

this is in contrast to the classical periodicity where the quantum  $\tau_m$  values do seem to more closely follow the classical prediction of Eqn. (8) and exhibit signs of the expected divergence as  $E \rightarrow +V_0$ . This term also provides the first estimate of the superrevival time as one no longer has  $E_m''' = 0$ ; this correction is somewhat akin to the introduction of a finite superrevival time in the finite well system [34], [35] when the well depth is not taken to infinity, yielding a non-quadratic dependence on quantum number.

While we are not aware of any corresponding explicit 4th-order calculation of the energy eigenvalues for the 'rotor in a field' system, one can make use of the perturbative expansion obtained by other methods in Eqn. (17) to write the equivalent of the 4th-order perturbation theory result in the form

$$E_m^{(4)} = \frac{V_0^2 I^2}{\hbar^6} \left[ \frac{20m^2 + 7}{(4m^2 - 1)^3 (4m^2 - 4)} \right] \quad (27)$$

and including these additional corrections does yield improved agreement with both the numerically evaluated energies (in Fig. 2) and in the prediction for the energy dependence of the classical period (in Fig. 3): it also sharpens the apparent 'dropoff' of the revival time as the energy approaches the separatrix value (as  $E \rightarrow +V_0$  from above) as illustrated in Fig. 4. Using the comparisons in Fig. 2 and 3, one can then better judge to what extent the predicted values for the revival times will likely reproduce the actual values for the complete quantum pendulum problem, as one approaches  $V_0$  from above. Henceforth, we will use the 4th-order predictions for the revival (and superrevival) times in comparisons to numerically obtained values for the pendulum system. We note that the leading (in  $m$ ) terms of the perturbation results in Eqns. (21), (26), and (27), as well as higher order ones in the detailed 'handbook' expansion in Eqn. (17) can be obtained in a very straightforward manner using the WKB approximation and we outline this procedure in Appendix A.

As a check on the standard assumption on the relative magnitudes of the various time scales in such problems, we can evaluate the lowest-order predictions for  $\tau$ ,  $T_{rev}$ , and  $T_{super}$ , using the relations in Eqn. (2). The zeroth-order energy in Eqn. (21) gives the leading contributions to the first two quantities, while the second-order term in Eqn. (26) gives the leading term for  $T_{super}$  and we find the hierarchy

$$T_{super} : T_{rev} : \tau = (4m^3/q)^2 : 2m : 1 \quad (28)$$

in the large  $m$  limit. We also recall that the next-to-leading corrections for each of these

quantities imply that  $\tau$  increases as  $E \rightarrow +V_0$ , while both  $T_{rev}, T_{super}$  decrease so that the time scales are compressed near the separatrix.

## V. LOW ENERGY HARMONIC OSCILLATOR LIMIT

In order to study the low-energy or oscillator-like limit of Eqn. (10), we write  $I = \mu l^2$  and expand the potential energy function for  $\theta \ll 1$ , giving

$$-\frac{\hbar^2}{2\mu l^2} \frac{d^2 \psi(\theta)}{d\theta^2} - V_0 \left( 1 - \frac{\theta^2}{2!} + \frac{\theta^4}{4!} - \frac{\theta^6}{6!} + \dots \right) \psi(\theta) = E \psi(\theta). \quad (29)$$

Collecting only the constant and quadratic terms from the potential energy, and writing  $x \equiv \theta l$  (again, in the spirit of a small angle approximation), we can write the exact Hamiltonian in the form

$$\hat{H}_0 + \hat{H}' = \hat{H}_0 + \sum_{r=2}^{\infty} \hat{H}_{2r} \equiv \left[ -\frac{\hbar^2}{2\mu} \frac{d^2}{dx^2} + \frac{1}{2} \left( \frac{V_0}{l^2} \right) x^2 - V_0 \right] + \sum_{r=2}^{\infty} (-1)^{r+1} \frac{V_0 x^{2r}}{(2r)! l^{2r}} \quad (30)$$

and we will treat the various  $\hat{H}_{2r}$  terms in  $\hat{H}'$  as perturbations. We next equate

$$\frac{1}{2} \mu \omega^2 \iff \frac{V_0}{2l^2} \quad \text{or} \quad \omega \equiv \sqrt{\frac{V_0}{ml^2}} = \sqrt{V_0/I} \quad (31)$$

so that the zeroth order energy eigenvalues are trivially given by

$$E_n^{(0)} = (n + 1/2) \hbar \omega - V_0 = (n + 1/2) \hbar \sqrt{V_0/I} - V_0. \quad (32)$$

Expressed in terms of  $a$  and  $q$ , this reduces to

$$a = -2q + 2(2n + 1)\sqrt{q} \quad (33)$$

which are the two leading terms of the 'handbook' expansion in Eqn. (19). This harmonic oscillator approximation is compared to the numerically obtained quantum pendulum eigenvalues in Fig. 2 (as crosses) as the leading (zeroth) order prediction, for  $E < +V_0$ . The classical periodicity from Eqn. (2) is given by

$$\tau_n = \frac{2\pi \hbar}{|E'_n|} = \frac{2\pi}{\omega} \quad (34)$$

and we superimpose these zeroth order predictions for  $(E_n, \tau_n)$  on the classical prediction of Eqn. (7) in Fig. 5 (as crosses).

The leading correction in this approach comes from treating  $\hat{H}_4$  using first-order perturbation theory to write

$$E_n^{(1)} = \langle n | \hat{H}_4 | n \rangle = -\frac{V_0}{4!l^4} \langle n | x^4 | n \rangle = -\frac{1}{4!} \frac{V_0}{l^4} \left[ \frac{3\hbar^2}{4\mu^2\omega^2} (2n^2 + 2n + 1) \right] \quad (35)$$

using elementary textbook results for the expectation value of  $x^4$  in oscillator states. As always, the evaluation of the expectation value of powers of  $x$  is most easily done using raising and lower operator formalism, with

$$x = \sqrt{\frac{\hbar}{2\mu\omega}} (\hat{A} + \hat{A}^\dagger) \quad (36)$$

where

$$\hat{A}|n\rangle = \sqrt{n}|n-1\rangle \quad \text{and} \quad \hat{A}^\dagger|n\rangle = \sqrt{n+1}|n+1\rangle \quad (37)$$

and we use this method in all our calculations below. Using the identification in Eqn. (31), we find that this reduces to

$$E_n^{(1)} = -\frac{\hbar^2}{32I} (2n^2 + 2n + 1). \quad (38)$$

In terms of  $a, q$ , this contributes a  $V_0$ -independent correction of the form

$$a^{(1)} = -\frac{(4n^2 + 4n + 2)}{8} = -\frac{(p^2 + 1)}{8} \quad (39)$$

where  $p = 2n + 1$ , which is the  $q$ -independent term in Eqn. (19).

This correction, arising from the anharmonicity of the potential, not only provides an improved prediction for the energy-period relationship in Fig. 5, but is also important as it gives the lowest-order prediction for the revival period in the low-energy limit, as in Refs. [28] and [29]. The revival time is given by

$$T_{rev} = \frac{2\pi\hbar}{|E_n''/2|} = \frac{32\pi I}{\hbar} \quad (40)$$

which is independent of  $V_0$  and 8 times the lowest-order result for the revival time for the pure rotor system from Eqn. (25). Thus, the revival time in the low-energy limit is predicted in terms of physical parameters of the systems, by the very specific anharmonicity arising from the form of the  $\cos(\theta)$  potential.

We show this first non-vanishing prediction for the revival time in the low-energy, oscillator like limit in Fig. 6 (as diamonds.) At this order, the superrevival time is formally infinite since the spectrum is still approximately quadratic in  $n$ .

At next order, one obtains two contributions, one from including the effect of  $\hat{H}_6$  in first order perturbation theory, and a second from using  $\hat{H}_4$  in second-order. The results can be written in the forms

$$E_n^{(2,a)} \equiv \langle n | \hat{H}_6 | n \rangle = + \frac{V_0}{6!l^6} \langle n | x^6 | n \rangle = \frac{V_0}{6!l^6} \left( \frac{\hbar}{2\mu\omega} \right)^3 5(4n^3 + 6n^2 + 8n + 3) \quad (41)$$

and

$$\begin{aligned} E_n^{(2,b)} &= \sum_{j \neq n} \frac{\langle n | \hat{H}_4 | j \rangle \langle j | \hat{H}_4 | n \rangle}{(E_n^{(0)} - E_j^{(0)})} \\ &= \left( -\frac{V_0}{4!l^4} \right)^2 \frac{1}{\hbar\omega} \sum_{j \neq n} \frac{\langle n | x^4 | j \rangle \langle j | x^4 | n \rangle}{(n - j)} \\ &= \left( -\frac{V_0}{4!l^4} \right)^2 \left[ \frac{-2}{\hbar\omega} \right] \left( \frac{\hbar}{2\mu\omega} \right)^4 (34n^3 + 51n^2 + 59n + 21) \end{aligned} \quad (42)$$

Again, using  $\omega = \sqrt{V_0/I}$  we then find the total second-order contribution to be

$$E_n^{(2)} = E_n^{(2,a)} + E_n^{(2,b)} = -\frac{\hbar^3}{I^2} \sqrt{\frac{I}{V_0}} \frac{(2n^3 + 3n^2 + 3n + 1)}{512} \quad (43)$$

which agrees (when expressed in terms of  $a$  and  $q$ ) with the expansion in Eqn. (19) and improves agreement with the 'exact' (numerically evaluated) pendulum values as shown in Fig. 2. The  $(E_n, \tau_n)$  values including these corrections are also plotted in Fig. 5 and similarly show improved agreement in the  $E < +V_0$  regime. In analogy to the high-energy rotor case, the lowest-order prediction of a fixed value of the revival time in this limit, in Eqn. (40) is changed in the next order so that  $T_{rev}$  decreases as  $E \rightarrow +V_0$  from below.

We can proceed in an identical (if increasingly more difficult) fashion to find the 3rd and 4th order corrections, namely

$$E_n^{(3)} = -\frac{\hbar^4}{V_0 I^2} \frac{(5n^4 + 10n^3 + 16n^2 + 11n + 3)}{8192} \quad (44)$$

$$E_n^{(4)} = -\frac{\hbar^5}{I^{5/2} V_0^{3/2}} \frac{(66n^5 + 165n^4 + 370n^3 + 390n^2 + 225n + 53)}{2^{19}} \quad (45)$$

and some of the details of their calculation are presented in Appendix B. In each case, the results match the 'handbook' expansion from Eqn. (19); they also improve agreement with numerically obtained values (as in Fig. 2) and with the classical periodicity (in Fig. 5), as well as steepening the 'dropoff' of the predicted quantum revival time in this limit as shown in Fig. 6. We see that the quantum revival times decrease (at least initially) as one goes

up in energy, in contrast to the quantum periods ( $\tau_n$ ) which increase in accordance (again, initially) with the classical prediction as one approaches the classical divergence in  $\tau$ .

We can also check the hierarchy of time scales, as done at the end of Sec. IV, in the low-energy limit. In this case, the lowest-order predictions for  $\tau$ ,  $T_{rev}$ , and  $T_{super}$  come from Eqns. (32), (38), and (43) respectively and give the simple ratios

$$T_{super} : T_{rev} : \tau = (8\sqrt{q})^2 : (8\sqrt{q}) : 1 \quad (46)$$

and higher-order corrections lead to increasing (decreasing) values of  $\tau$  ( $T_{rev}, T_{super}$ ) as  $E \rightarrow +V_0$  as in the high-energy rotor limit, with the various time scales being 'compressed' near the separatrix.

## VI. CLASSICAL PERIODICITY, REVIVAL AND SUPERREVIVAL TIMES FOR THE PENDULUM

We have derived perturbative expressions for the quantized energies in both the low- and high-energy limits, and can therefore evaluate approximate expressions for all of the relevant time scales in Eqn. (2), as well as judging their relevant range of validity by comparing to 'exact' values as in Fig. 1. In order to examine the behavior of the classical periods, and revival and superrevival times, near the separatrix (for  $E \approx +V_0$ ) where neither approximation scheme is applicable, we need to use numerically obtained values. With the energy spectrum,  $E_n$  versus  $n$ , obtained in this way, we can approximate the required derivatives with respect to quantum number by making associations such as

$$\frac{dE_n}{dn} \implies \frac{\Delta E_n}{\Delta n} = E_{n+1} - E_n \quad \text{and} \quad \frac{d^2 E_n}{dn^2} \implies \frac{\Delta^{(2)} E_n}{\Delta n^2} = E_{n+1} - 2E_n + E_{n-1} \quad (47)$$

with similar expressions for higher order derivatives. However, because of the degeneracy between even and odd rotor-like states in the high energy limit, if we simply enumerate all of the allowed states in some standard ordering, we find vanishing 'derivatives' in the free rotor limit which are artifacts. In the construction of a general, high-energy wave packet, one would find approximately equal contributions from both the (almost exactly degenerate) even ( $ce_{2m}$ ) and odd ( $se_{2m}$ ) solutions which would be only 'counted' once. To avoid this difficulty, we can classify the states by their parity and evaluate the approximate derivatives in Eqn. (47) separately in both the even and odd cases. For the low-energy, oscillator limit,

this means that we 'sample' every other state and so, for example, obtain first-derivative type terms which are a factor of two too small (since effectively we have used  $\Delta n = 2$  instead of  $\Delta n = 1$ ), with a similar factor of 4 for the second derivative term. This procedure is not as artificial as it may seem, since one can imagine constructing wave packets of definite parity, even or odd, at appropriate points of symmetry for the pendulum (either at  $\theta = 0$  or  $\theta = \pi$ ) which would then have contributions only from the even or odd parity eigensolutions.

Following this procedure, we construct approximations for the first derivatives by generalizing Eqn. (47) slightly by associating the 'average' energy

$$\overline{E}_n = \frac{1}{2}(E_{n+1} + E_n) \quad \text{with} \quad \frac{\Delta E_n}{\Delta n} = E_{n+1} - E_n \equiv \Delta E_n \quad (48)$$

so that we associate

$$\overline{E}_n \quad \text{and} \quad \overline{\tau}_n = \frac{2\pi\hbar}{|\Delta E_n|}. \quad (49)$$

We plot, in Fig. 7, both the even-parity (crosses) and odd-parity (diamonds) values for  $(\overline{E}_n, \overline{\tau}_n)$  obtained in this way. (Note that the values for  $E < +V_0$  are shown on an appropriately scaled (factor of 2) axis, compared to those values for  $E > +V_0$ .) We note that the 'exact' data do closely follow the classical curves from Eqns. (7) and (8), and do exhibit a large, but finite peak at  $E \approx +V_0$ , in both sets of data. The lack of a true divergence is understandable given the quantized nature of the energy eigenvalues and has been discussed in terms of the explicit time evolution of wave packet solutions as described in Ref. [7], which also outlines simple uncertainty principle arguments.

Turning now to the question of the behavior of the revival time as  $E \rightarrow +V_0$  (from either above or below), while there is no classical prediction comparable to that for  $\tau(E)$  versus  $E$ , we can make use of the 4th-order perturbative results to evaluate  $T_{rev} = 2\pi\hbar/|E_n''/2|$  versus  $E_n$  which will give good representations in both the low- and high-energy limits. Using the 4th-order results plotted in Figs. 3 and 5, we produce the limiting predictions for  $T_{rev}$  versus  $E_n$ , shown as solid curves, in Fig. 8. The numerically obtained 'exact' results, using the prescription in Eqn. (47), are also shown in Fig. 8, again with the low-energy 'data' ( $E < +V_0$ ) shown scaled, now by a factor of 4. Once again, the agreement with the perturbative predictions in the two limits is good, with  $T_{rev}$  clearly decreasing from the appropriate  $E \ll +V_0$  and  $E \gg +V_0$  limits until very near  $E \approx +V_0$  where it reaches a large, but finite value. Similar results can be seen for the superrevival time,  $T_{super}$ , comparing the predictions from 4th-order perturbation theory in both the low- and high-energy limits

with discretized derivatives of the numerically obtained results (appropriately scaled for  $E < +V_0$ ), yielding plots which are quite similar to Fig. 8.

## VII. DISCUSSION AND CONCLUSIONS

We have examined the quantized energy eigenvalue spectrum of the quantum pendulum problem, focusing on information about the classical periodicity and quantum revivals and superrevivals. Using 4th-order perturbative approximations for the low-energy (oscillator) and high-energy (rotor) limits of the pendulum, we have found good agreement with numerically obtained eigenvalues. This has allowed us to derive expressions for the revival and superrevival times in these limits, as well as to establish limits on their validity. The revival times for the pendulum decrease from constant values, proportional to  $\hbar/I$ , as one approaches the separatrix from both above and below. Near the separatrix, we have used numerically obtained values to show that the classical period exhibits a large, but finite value at  $E \approx +V_0$ , while the revival times also increase (very near this value).

This problem is an interesting example of a quantum system which exhibits a rich variety of classical periodicities and quantum revival and superrevival times, all of which are perturbatively calculable in limiting cases, as well as classically divergent behavior at a special value, which is 'softened' by quantum effects. The behavior of the time scales as they near the critical value at the separatrix, where they can be clearly seen to compress towards each other as  $E \rightarrow +V_0$ , differs from the pattern seen in other systems with quantum revivals. One can speculate on possible experimental realizations of such behavior in systems exhibiting hindered internal rotations [2] - [5].

The energy level structure of the quantum pendulum is, to a large extent, determined by the numerical (and dimensionless) value of  $q$  and we can discuss order-of-magnitudes estimates for  $q$  for some model systems, and how they scale with the physical parameters involved. In the classical limit of a macroscopic pendulum system under the influence of gravity, with  $m \sim 1 \text{ kg}$  and  $l \sim 1 \text{ m}$ , we find  $q \sim 10^{70}$  so that there is the expected huge number of oscillatory states below the separatrix and one is clearly in the correspondence principle limit. At the other extreme, for an electron ( $m_e$ ) restricted to a radius characteristic of that of a carbon nanotube ( $L \sim 1 \text{ nm}$ ), under the influence of gravity, we find that  $q \sim 10^{-18}$  and the system is automatically in the high-energy or free-rotor limit. In this



case, the revival time should be given to an excellent approximation by Eqn. (25), with no corrections due to the external potential, as well as having  $T_{super} \rightarrow \infty$ . For the more interesting case of an electron (or ion) subject to an electric field of order  $E_0 = 100 V/m$ , we find  $q \sim 10^{-6}(M/m_e)(E/E_0)(l/1 nm)^3$  so that for electrons in such fields the high-energy free rotor limit is also applicable. On the other hand, for ions ( $M/m_e > 10^4$ ) in strong fields ( $E > 10^5 V/m$ ) in larger diameter ( $L > 10 nm$ ) geometries, one has  $q \sim 10^4$  and an interesting number of vibrational states could be present. This range is perhaps more typical of that explored in studies of hindered internal rotations [2] -[4]. We have found that the revival times, in both the high-energy (Eqn. (25)) and low-energy (Eqn. (40)) limits scale as  $T_{rev} \propto I/\hbar$ , which gives numerical values in the range,  $T_{rev} \sim (100 fs - 1000 fs) (M/m_e)(l/1 nm)^2$ , independent of the pendulum potential,  $V_0$ .

A simple extension of this system would be to consider a particle confined to a circular (radius  $l$ ) cylinder of length  $L$ , subject to a field perpendicular to the central axis. This separable system would then have quantized energies consisting of the quantum pendulum values discussed here plus a term given by  $E_k^{(z)} = \hbar^2 k^2 / 2\mu L^2$  corresponding to the quantized motion along the cylinder. The pattern of classical periodicities and quantum revivals in systems characterized by two quantum numbers has been discussed [36], [37]. A more careful study of this case might be motivated by its possible realization in the geometry of carbon nanotubes. A related two-dimensional generalization would be to consider the point object restricted to the surface of a sphere which has a richer set of possible classical motions.

### Acknowledgments

This work was supported in part by the National Science Foundation under Grant DUE-9950702. One of us (R. W. R.) also thanks H. Kaplan for conversations regarding aspects of this problem as well as the organizers of the 2002 Gordon Conference on Physics Research and Education (Quantum Mechanics) for their hospitality.

## APPENDIX A: WKB APPROXIMATION SOLUTIONS TO THE MATHIEU EQUATION

We briefly describe in this Appendix a simple WKB-based approximation which gives the leading order (in  $m$ ) results for the (approximately degenerate) characteristic values,  $a_r, b_r$ , in the high-energy limit (rotor-like) of the quantum pendulum problem, as an expansion in powers of  $V_0$ . In this context, it reproduces the leading  $m$  behavior of well-known 'handbook' results in Refs. [32] and [33] for the characteristic values  $a_m, b_m$  in terms of the parameter  $q$ , in a very straightforward way.

We first rewrite the classical energy conservation connection

$$\frac{p_\theta^2}{2I} - V_0 \cos(\theta) = E \quad (\text{A1})$$

in the form

$$p_\theta = \sqrt{2I} \sqrt{E + V_0 \cos(\theta)}. \quad (\text{A2})$$

In the spirit of a WKB approach, we quantize the integral of  $p_\theta$  in the form

$$\sqrt{2I} \int_{-\pi}^{+\pi} \sqrt{E + V_0 \cos(\theta)} d\theta = \int_{-\pi}^{+\pi} p_\theta d\theta = m\pi\hbar. \quad (\text{A3})$$

For the physical situation of the quantum pendulum, we would restrict ourselves to even values of  $m$ , but for comparison to the general result inspired by Mathieu equations, we allow any integral  $m$  values. In terms of the Mathieu equation parameters in Eqn. (13) we can write this in the form

$$2m\pi = \sqrt{a} \int_{-\pi}^{+\pi} \left(1 + \frac{2q}{a} \cos(\theta)\right)^{1/2} d\theta \quad (\text{A4})$$

One can expand the integrand as a series in  $q/a$  and perform the angular integrals, leaving only the even terms present, to obtain

$$m = \sqrt{a} \left(1 - \frac{q^2}{4a^2} - \frac{15q^4}{64a^2} - \frac{105q^6}{256a^6} + \dots\right) \quad (\text{A5})$$

or

$$a = m^2 \left(1 - \frac{q^2}{4a^2} - \frac{15q^4}{64a^2} - \frac{105q^6}{256a^6} + \dots\right)^{-2}. \quad (\text{A6})$$

This can be solved recursively in powers of  $q^2$  to obtain the approximation solution

$$a_m = m^2 + \frac{q^2}{2m^2} + \frac{5q^4}{32m^6} + \frac{9q^6}{64m^{10}} + \dots. \quad (\text{A7})$$

and this form agrees with the handbook results of Refs. [32] and [33]. One can then easily extend this result (again to leading order in  $m$ ) to quite high order.

**APPENDIX B: THIRD- AND FOURTH-ORDER PERTURBATION THEORY  
RESULTS IN THE OSCILLATOR LIMIT**

For the third-order correction to the low-energy, harmonic oscillator limit, we need to evaluate three distinct contributions, namely, (i) the  $\hat{H}_8$  term in first order, (ii) the  $\hat{H}_6$  and  $\hat{H}_4$  terms (in both orders) in second order, and (iii) the  $\hat{H}_4$ ,  $\hat{H}_4$ ,  $\hat{H}_4$  terms in third order. For example, the first contribution is

$$-\frac{V_0}{l^8 8!} \langle n|x^8|n \rangle = - \left[ \frac{\hbar^2}{I^2 V_0} \right] \frac{5(14n^4 + 28n^3 + 70n^2 + 56n + 21)}{8! 2^4} \quad (\text{B1})$$

The expression for the third-order energy shift is presented in some elementary texts, but we reproduce it below for completeness, specifically

$$E_n^{(3)} = \sum_{j \neq n} \sum_{l \neq n} \frac{\langle n|\hat{H}'|j \rangle \langle j|\hat{H}'|l \rangle \langle l|\hat{H}'|n \rangle}{(E_n^{(0)} - E_j^{(0)})(E_n^{(0)} - E_l^{(0)})} - \langle n|\hat{H}'|n \rangle \sum_{j \neq n} \frac{\langle n|\hat{H}'|j \rangle \langle j|\hat{H}'|n \rangle}{(E_n^{(0)} - E_j^{(0)})^2} \quad (\text{B2})$$

Including all three sets of terms, we obtain the result shown in Eqn. (44).

For the increasingly complex matrix algebra involved in the evaluation of such terms, we make use of symbolic manipulation programs (in our case *Mathematica*<sub>®</sub>) and write

$$\langle i|x|j \rangle = \sqrt{\frac{\hbar}{2\mu\omega}} \langle i|\hat{A} + \hat{A}^\dagger|j \rangle = \sqrt{\frac{\hbar}{2\mu\omega}} \left[ \sqrt{j} \delta_{i,j-1} + \sqrt{j+1} \delta_{i,j+1} \right] \quad (\text{B3})$$

and evaluate the required matrix elements of higher powers by repeated matrix multiplication. We note that in third-order (and beyond) in perturbation theory, there are consistently terms including factors of the form  $\langle n|\hat{H}'|n \rangle$ . At third-order, and beyond, in intermediate steps of the calculation, the individual expressions one obtains may be of higher order (in  $n$ ) than are present in the final result, and the presence of such cancellations can be used as a check on the internal consistency of the calculation.

Finally, for the 4th-order terms, we require the contributions from (i)  $\hat{H}_{10}$  in first order, (ii)  $\hat{H}_8$ ,  $\hat{H}_4$  (both orderings) in second order, (iii)  $\hat{H}_6$ ,  $\hat{H}_6$ , also in second order, (iv),  $\hat{H}_6$ ,  $\hat{H}_4$ ,  $\hat{H}_4$  (three orderings) in third order, and (v)  $\hat{H}_4$ ,  $\hat{H}_4$ ,  $\hat{H}_4$ ,  $\hat{H}_4$  in 4th-order. The explicit expression for the energy shift in 4th order, in terms of unperturbed wavefunctions and energies, is less

often seen (see, *e.g.*, [38]) so we also reproduce it here for completeness.

$$\begin{aligned}
E_n^{(4)} = & \sum_{j \neq n} \sum_{l \neq n} \sum_{r \neq n} \frac{\langle n | \hat{H}' | j \rangle \langle j | \hat{H}' | l \rangle \langle l | \hat{H}' | r \rangle \langle r | \hat{H}' | n \rangle}{(E_n^{(0)} - E_j^{(0)})(E_n^{(0)} - E_l^{(0)})(E_n^{(0)} - E_r^{(0)})} \\
& - \langle n | \hat{H}' | n \rangle \sum_{j \neq n} \sum_{l \neq n} \frac{\langle n | \hat{H}' | j \rangle \langle j | \hat{H}' | l \rangle \langle l | \hat{H}' | n \rangle}{(E_n^{(0)} - E_j^{(0)})(E_n^{(0)} - E_l^{(0)})^2} \\
& - \langle n | \hat{H}' | n \rangle \sum_{j \neq n} \sum_{l \neq n} \frac{\langle n | \hat{H}' | j \rangle \langle j | \hat{H}' | l \rangle \langle l | \hat{H}' | n \rangle}{(E_n^{(0)} - E_j^{(0)})^2 (E_n^{(0)} - E_l^{(0)})} \\
& + \langle n | \hat{H}' | n \rangle \langle n | \hat{H}' | n \rangle \sum_{j \neq n} \frac{\langle n | \hat{H}' | j \rangle \langle j | \hat{H}' | n \rangle}{(E_n^{(0)} - E_j^{(0)})^3} \\
& - \left[ \sum_{r \neq n} \frac{\langle n | \hat{H}' | r \rangle \langle r | \hat{H}' | n \rangle}{(E_n^{(0)} - E_r^{(0)})} \right] \left[ \sum_{j \neq n} \frac{\langle n | \hat{H}' | j \rangle \langle j | \hat{H}' | n \rangle}{(E_n^{(0)} - E_j^{(0)})^2} \right]
\end{aligned} \tag{B4}$$

As a cross-check of our more automated approach to the 3rd and 4th order calculations, we have followed the same approach for the 1st- and 2nd-order results and confirm that we reproduce the values in Eqns. (38) and (43). Perhaps more interestingly, we also note that there are three simple extensions of the 'basic' oscillator, defined by the zeroth-order potential  $V(x) = \mu\omega^2 x^2/2$ , which can be used as benchmarks for such higher order calculations. First of all, the addition of a constant perturbing potential term,  $V'_0$ , should only affect the energy spectrum through the first-order correction  $E_n^{(1)} = \langle n | V'_0 | n \rangle = V'_0$  and one can easily check that all higher order corrections vanish in this case.

The inclusion of a linear term of the form  $V'(x) = -Fx$  can be solved exactly by completing the square giving

$$V(x) = \frac{1}{2}\mu\omega^2 x^2 - Fx = \frac{1}{2}\mu\omega^2 \left( x - \frac{F}{\mu\omega^2} \right)^2 - \frac{F^2}{2\mu\omega^2} = V(x - x_0) - \tilde{E}_0 \tag{B5}$$

to give  $E'_n = E_n - F^2/2\mu/\omega^2 = E_n - \tilde{E}_0$ . Thus, the inclusion of an  $\hat{H}' = -Fx$  perturbation should find a non-vanishing result only for  $E_n^{(2)}$  and we confirm this.

Finally, the inclusion of a small quadratic correction to the original oscillator potential by  $V'(x) = \lambda x^2$  leads to a simple redefinition of the oscillator frequency  $\omega' = \omega\sqrt{1 + 2\lambda/\hbar\omega^2}$  and the result

$$E'_n = (n + 1/2)\hbar\omega' = E_n \left( 1 + \frac{2\lambda}{\hbar\omega^2} \right)^{1/2} \tag{B6}$$

which can be expanded as an ordinary power series in  $\lambda$ . One can then compare this result to that obtained by evaluation of the first- through 4th-order perturbation results, including

those of Eqns. (B2) and (B4) and we find complete agreement.

---

- [1] E. U. Condon, *Phys. Rev.* **31**, 891 (1928).
- [2] D. G. Lister, J. N. MacDonald, and N. L. Owen, *Internal Rotation and Inversion* (Academic Press, London, 1978).
- [3] W. J. Orville-Thomas (editor), *Internal Rotation in Molecules*, (Wiley, New York, 1974).
- [4] G. Ercolani, *J. Chem. Ed.* **77**, 1495 (2000).
- [5] G. L. Baker, J. A. Blackburn, and H. J. T. Smith, *Am. J. Phys.* **70**, 525 (2002).
- [6] T. Pradhan and A. V. Khare, *Am. J. Phys.* **41**, 59 (1973).
- [7] G. P. Cook and C. S. Zaidins, *Am. J. Phys.* **54**, 259 (1986).
- [8] R. Aldrovandi and P. Leal Ferreira, *Am. J. Phys.* **48**, 660 (1980).
- [9] M. Schwartz and M. Martin, *Am. J. Phys.* **26**, 639 (1958).
- [10] G. L. Johnston and G. Sposito, *Am. J. Phys.* **44**, 723 (1976).
- [11] D. Kiang, *Am. J. Phys.* **46**, 1188 (1978).
- [12] F. Constantinescu and E. Magyari, *Problems in Quantum Mechanics* (Pergamon, Oxford, 1971), pp. 205, 209-210.
- [13] S. Flügge, *Practical Quantum Mechanics I* (Springer-Verlag, New York, 1974), pp. 110-112.
- [14] L. Pauling and E. B. Wilson, Jr., *Introduction to Quantum Mechanics, with Applications to Chemistry* (McGraw-Hill, New York, 1935), pp. 177-178.
- [15] S. B. Cahn, G. D. Mahan, and B. E. Nadgorny, *A Guide to Physics Problems: Part 2* (Plenum Press, New York, 1997), pp. 66-67, 289-291.
- [16] V. I. Kogan and V. M. Galitskiy, *Problems in Quantum Mechanics* (Prentice-Hall, Englewood Cliffs, 1963), pp. 14, 185-186.
- [17] J. A. Cronin, D. F. Greenberg, V. L. Telegdi, *University of Chicago Graduate Problems in Physics, with Solutions* (Addison-Wesley, Reading, 1967), pp. 31, 162.
- [18] For an excellent review of wave packet dynamics, see *The Physics and Chemistry of Wave Packets*, edited by J. A. Yeazell and T. Uzer (Wiley, NY, 2000).
- [19] G. Alber and P. Zoller, *Phys. Rep.* **199**, 231 (1991).
- [20] For Rydberg atoms, Z. D. Gaeta, M. W. Noel, and C. R. Stroud, Jr., *Phys. Rev. Lett.* **73**, 636 (1994); for Stark wave packets, R. Bluhm, V. A. Kostelecký, and B. Tudose, *Phys. Rev.* **A55**,

- 819 (1997); for alkali-metal atoms, R. Bluhm and V. A. Kostelecký, Phys. Rev. **A51**, 4767 (1995); for the effects of quantum defects, R. Bluhm and V. A. Kostelecký, Phys. Rev. **A50**, R4445 (1994); for the Jaynes-Cummings model, I. Sh. Averbukh, Phys. Rev. **A46**, R2205 (1992); for an atom in a gravity well; W. -Y. Chen and G. J. Milburn, Phys. Rev. **A51**, 2328 (1995); J. Gea-Banacloche, Am. J. Phys. **67**, 776 (1999), for aligned rotational wave packets, T. Seideman, Phys. Rev. Lett. **83**, 4971 (1999).
- [21] D. L. Aronstein and C. R. Stroud Jr, Phys. Rev. **A55**, 4526 (1997).
- [22] G. A. Vugalter, A. K. Das, and V. A. Sorokin, Phys. Rev. A **66**, 012104 (2002).
- [23] P. Stifter, W. E. Lamb Jr, and W. P. Schleich, in *Frontiers of Quantum Optics and Laser Physics*, Proceedings of the International Conference on Quantum Optics and Laser Physics (Springer, Singapore, 1997) edited by S. Y. Zhu, M. S. Zubairy, and M. O. Scully, pp. 236-246.
- [24] R. Bluhm, V. A. Kostelecký, and J. Porter, Am. J. Phys. **64**, 944 (1996).
- [25] R. W. Robinett, Am. J. Phys. **68**, 410 (2000).
- [26] D. F. Styer, Am. J. Phys. **69**, 56 (2001).
- [27] M. Auzinsh, Can. J. Phys. **77**, 491 (1999).
- [28] S. I. Vetchinkin and V. V. Eryomin, Chem. Phys. Lett. **222**, 394 (1994).
- [29] W. Loinaz and T. J. Newman, J. Phys. A: Math. Gen. **32**, 8889 (1999).
- [30] For fractional revivals of a molecular wave packet, see M. J. J. Vrakking, D. M. Villeneuve, and A. Stolow, Phys. Rev. A **54**, R37 (1996).
- [31] R. W. Robinett, J. Math. Phys. **41**, 1801 (2000).
- [32] N. W. McLachlan, *Theory and Application of Mathieu Functions*, (Oxford University Press, London, 1947).
- [33] M. Abramowitz and I. A. Stegun, *Handbook of Mathematical Functions*, (McGraw-Hill, New York, 1964), pp. 722-726.
- [34] A. Venugopalan and G. S. Agarwal, Phys. Rev. A **59**, 1413 (1999).
- [35] D. L. Aronstein and C. R. Stroud, Jr., Phys. Rev. A **62**, 022102 (2000).
- [36] R. Bluhm, V. Alan Kostelecký, and B. Tudose, Phys. Lett. **A222**, 220-226 (1996).
- [37] G. S. Agarwal and J. Banerji, Phys. Rev. **A57**, 3880 (1998).
- [38] See, *e. g.* J. O. Hirschfelder, W. B. Brown, and S. T. Epstein, in *Advances in Quantum Chemistry*, Vol. 1 (Academic Press, New York, 1964), pp. 256-268.

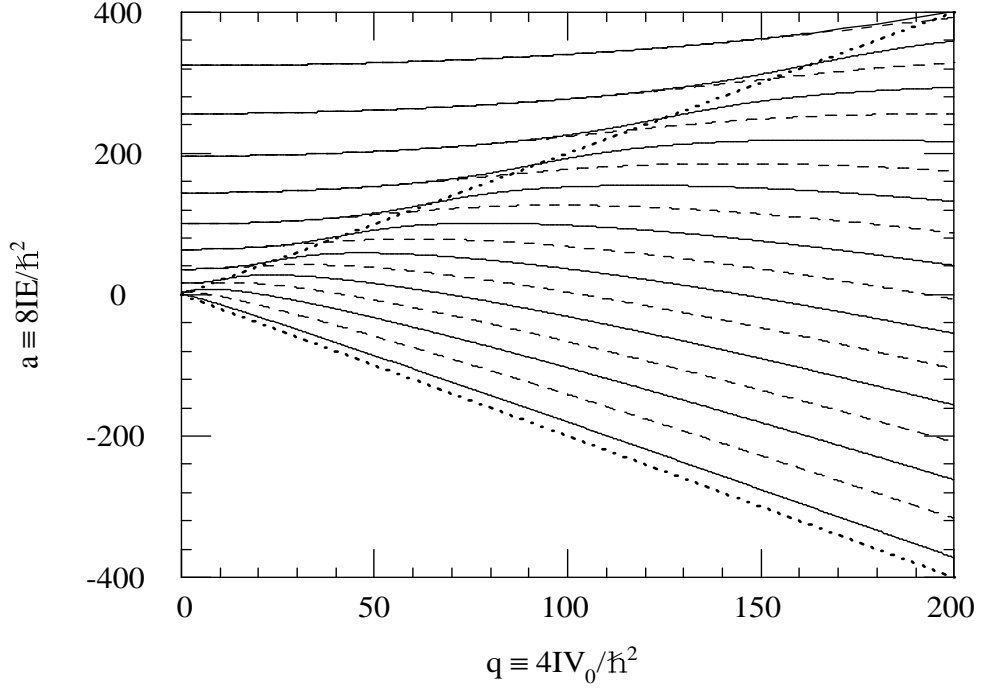


FIG. 1: Plots of the characteristic values for the Mathieu equation,  $a_{2m}$  (for even solutions, solid curves) and  $b_{2m}$  (for odd solutions, dashed curves) versus  $q$  for the quantum pendulum. The dotted lines correspond to  $a = \pm 2q$  or  $E = \pm V_0$ . Note that for a given value of  $q$  (at least for  $a \ll q$ ) that the gap between the lowest energy state (lowest solid curve) is roughly one-half of the spacing between solid and dashed curves, corresponding to the zero-point energy in the oscillator limit.

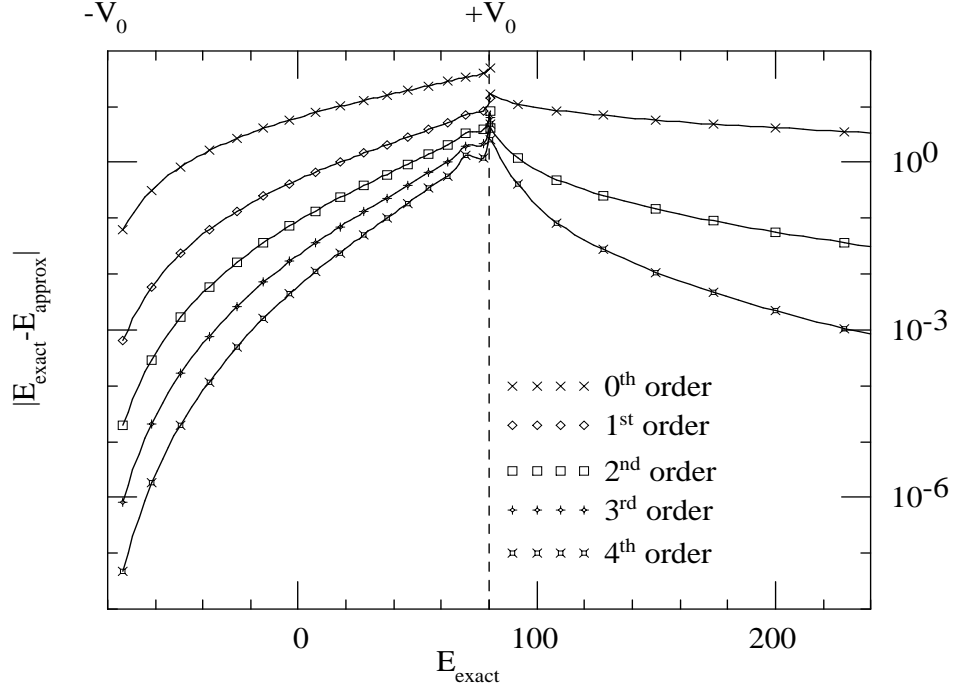


FIG. 2: Plots of the difference between the perturbative approximations for the energy eigenvalues and the 'exact' values (from direct numerical evaluation) in various orders of perturbation theory. The parameter values in Eqn. (20) are used. For the  $E > +V_0 = 80$  cases (using the high energy rotor limit) the zeroth, second, and 4th-order expressions in Eqns. (21), (26), and (27) are used. For the  $E < +V_0$  case, the low-energy oscillator approximations in Eqns. (32), (38), (43), (44), and (45) are used.



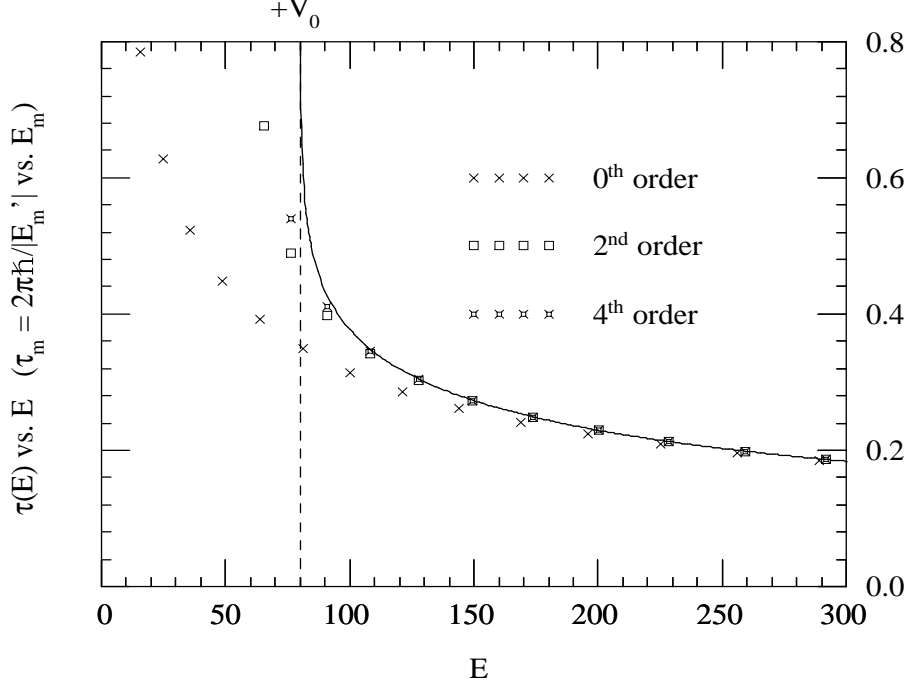


FIG. 3: Plots of  $\tau(E)$  versus  $E$  for the classical pendulum from Eqn. (8) (solid curve) and of the equivalent quantum values,  $\tau_m \equiv 2\pi\hbar/|E'_m|$  versus  $E_m$  using zeroth- (from Eqn. (21), as crosses), second- (from Eqn. (26), as squares), and 4th-order (from Eqn. (27), as stars) perturbation theory.

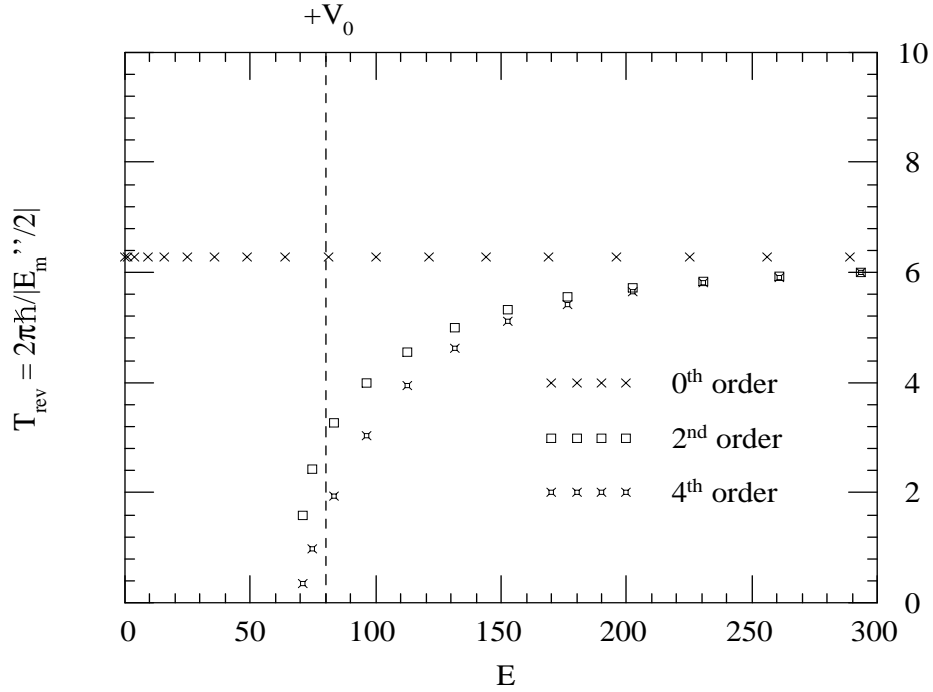


FIG. 4: Plots of the revival time  $T_{rev}$  versus  $E$  using  $T_{rev} \equiv 2\pi\hbar/|E''_m/2|$  in zeroth-, second-, and 4th-order perturbation theory (with the same notation as Fig. 3.)

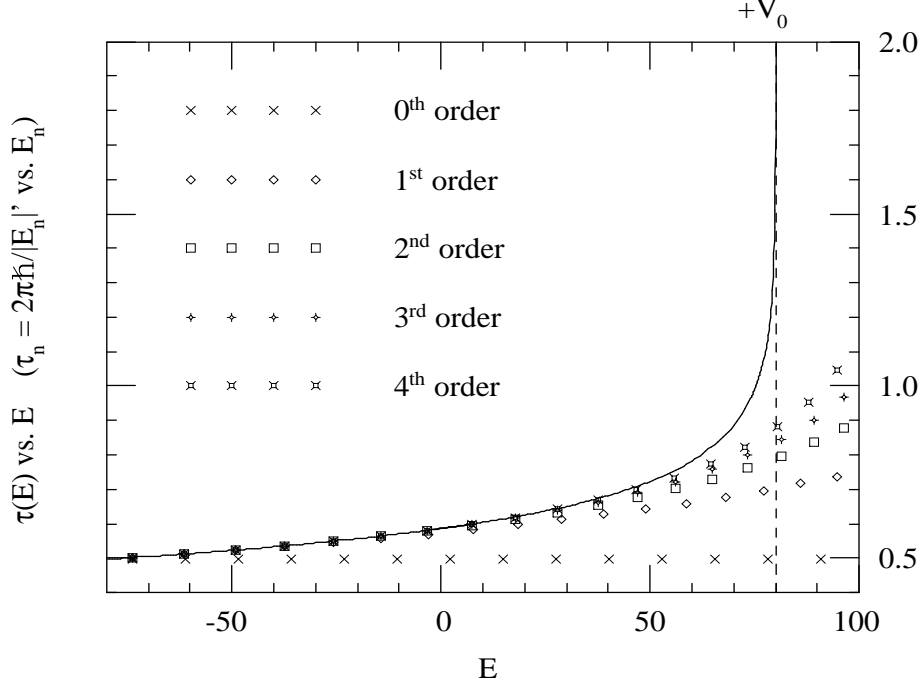


FIG. 5: Plots of  $\tau(E)$  versus  $E$  for the classical pendulum from Eqn. (7) (solid curve) and of the equivalent quantum values,  $\tau_m = 2\pi\hbar/|E'_m|$  versus  $E_m$  using zeroth (from Eqn. (32), as crosses), first (from Eqn. (38), as diamonds), second (from Eqn. (43), as squares), third (from Eqn. (44), as bursts), and 4th order (from Eqn. (27), as stars) perturbation theory.

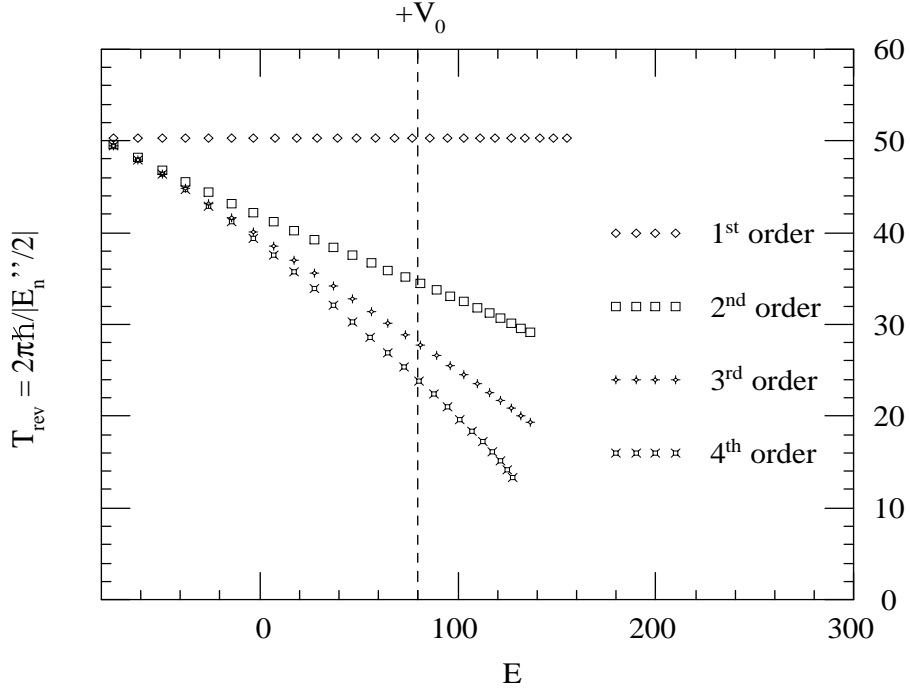


FIG. 6: Plots of the revival time  $T_{rev}$  versus  $E$  using  $T_{rev} \equiv 2\pi\hbar/|E''_m/2|$  in first-, second-, third-, and 4th-order perturbation theory (with the same notation as Fig. 5.)

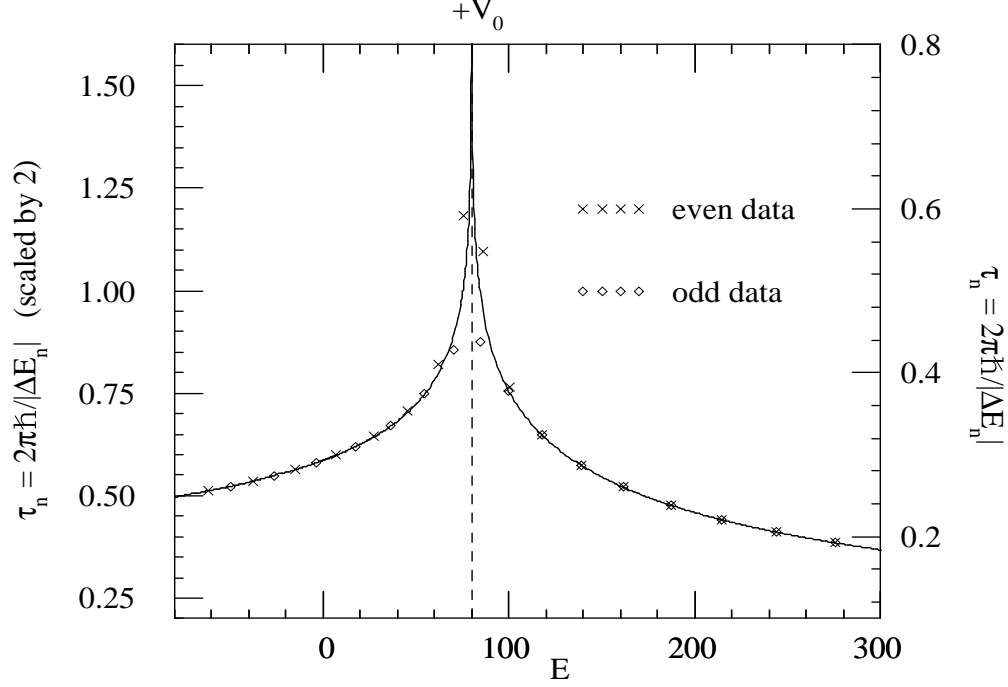


FIG. 7: Plot of  $\tau_n \equiv 2\pi\hbar/|\Delta E_n|$  versus  $E_n$  for the parameters in Eqn. (20) for even (crosses) and odd (diamonds) energy eigenvalues. The classical expressions for  $\tau(E)$  versus  $E$  from Eqns. (7 and (8) are used.

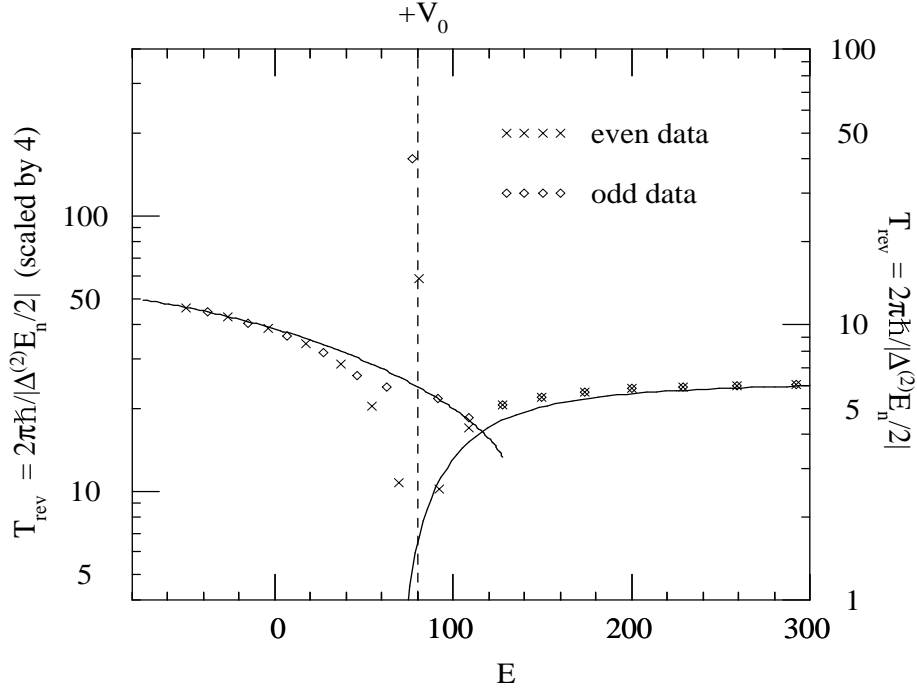


FIG. 8: Plot of the revival times  $T_{rev} \equiv 2\pi\hbar/|\Delta^{(2)} E_n/2|$  versus  $E_n$  for the parameters in Eqn. (20) for even (crosses) and odd (diamonds) energy eigenvalues. The solid curves are the predictions using 4th-order perturbation theory from the respective limiting cases.